

New cross section data and review of production routes of medically used ^{110m}In

F. Tárkányi^a, S. Takács^a, F. Ditrói^{a,*}, A. Hermanne^b, M. Baba^c, B.M.A. Mohsena^d, A.V. Ignatyuk^e

^a*Institute for Nuclear Research, Hungarian Academy of Sciences (ATOMKI), Debrecen, Hungary*

^b*Cyclotron Laboratory, Vrije Universiteit Brussel (VUB), Brussels, Belgium*

^c*Cyclotron Radioisotope Center (CYRIC), Tohoku University, Sendai, Japan*

^d*Nuclear Research Center Egyptian Atomic Energy Authority, Cairo, Egypt*

^e*Institute of Physics and Power Engineering (IPPE), Obninsk, Russia*

Abstract

Evaluation of nuclear data for production routes of ^{110m}In is in progress in the frame of an IAEA Coordinated Research Project (CRP). New experimental cross section data for the indirect $^{nat}\text{In}(p,x)^{110}\text{Sn} \rightarrow ^{110m}\text{In}$ and for the direct $^{107}\text{Ag}(\alpha,n)^{110m}\text{In}$ and $^{109}\text{Ag}(^3\text{He},2n)^{110m}\text{In}$ production routes and for the satellite impurity reactions $^{107}\text{Ag}(\alpha,xn)^{110g,109}\text{In}$ and $^{109}\text{Ag}(^3\text{He},xn)^{110g,111,109}\text{In}$ have been measured by using the activation method, stacked foil irradiation technique and gamma-ray spectrometry. Additional data are reported for production of the ^{111}In diagnostic gamma-emitter via the $^{109}\text{Ag}(\alpha,2n)^{111}\text{In}$ reaction. The earlier experimental data were critically reviewed in order to prepare recommended data and optimal production parameters for the different routes.

Keywords: Indium-110m, medical radioisotopes, charged particle reactions

1. Introduction

Various radiopharmaceuticals, labeled with ^{111}In ($T_{1/2} = 2.81$ d, 100 % EC decay) are used in the diagnosis of cancer and other diseases through SPECT. However, in particular for receptor-type studies, the quantification of the uptake of the radiopharmaceutical via PET measurements might be important. For ^{111}In the corresponding isotope of choice is ^{110m}In . This metastable state with $I^\pi = 2^+$ has a half-life of 69.1 min and decays in 61.25 % via positron emission with $E_{max} = 2.3$ MeV. Evaluation of nuclear data for production routes of ^{110m}In is performed in the frame of an IAEA Coordinated Research Project [1]. The task was assigned to the ATOMKI-VUB group, which previously already published results for some related reactions [2–9]. As the compilation of all earlier experimental studies showed a lack of data and in some cases large disagreements, we decided to re-investigate the most promising reactions. Two basic routes exist for production of ^{110m}In : a direct and an indirect process. The principal reactions of direct production, with limited contaminants, are $^{110}\text{Cd}(p,n)$, $^{110}\text{Cd}(d,2n)$, $^{107}\text{Ag}(\alpha,n)$ and $^{109}\text{Ag}(^3\text{He},2n)$. The direct production of ^{110m}In always leads to the co-formation of

the ground state ^{110g}In ($I^\pi = 7^+$, $T_{1/2} = 4.9$ h). This co-formation increases with increasing projectile energy because of the higher spin of the ground state, but it cannot be observed in all cases of our investigations. In all cases, in order to minimize the impurity level, highly enriched targets should be used and the covered energy range should be optimized, which requires information on the production of the disturbing, simultaneously produced, longer-lived ^{109}In , ^{110g}In and ^{111}In radioisotopes. Isotopically pure ^{110m}In could only be prepared via the generator system ^{110}Sn ($T_{1/2} = 4.11$ h, EC 100 %) \rightarrow ^{110m}In . The mother isotope of the generator (^{110}Sn) could be obtained at low and medium energies with light charged particles via the $^{113}\text{In}(p,4n)$, $^{113}\text{In}(d,5n)$, $^{110}\text{Cd}(^3\text{He},3n)$, $^{108}\text{Cd}(\alpha,2n)$ and $^{110}\text{Cd}(\alpha,4n)$ reactions. Disturbing co-produced radioisotopes, requiring optimization of the energy range and use of enriched targets, are the long-lived ^{113g}Sn , decaying to ^{113m}In and finally to stable ^{113}In (hence decreasing specific activity), and the rather short-lived ^{111}Sn ($T_{1/2} = 35.3$ min) decaying to ^{111}In ($T_{1/2} = 2.81$ d).

2. Experimental

The general characteristics and procedures for irradiation, activity assessment and data evaluation (including estimation of uncertainties) were similar to many of our

*Corresponding author: ditroi@atomki.hu

earlier works [10, 11]. The main experimental parameters and the methods of data evaluation for the present study are summarized in Table 1. The used decay data are collected in Table 2.

3. Experimental results

We are reporting cross sections for production of ^{110m}In , ^{109}In , ^{110g}In and ^{111}In in Ag targets irradiated with ^3He and alpha particles. The last three radioisotopes are important from the point of view of radionuclide purity in the case of direct production of ^{110m}In . For the experiments on In targets, proton induced cross section data for production of the mother isotope ^{110}Sn are reported and data for the shorter-lived, co-produced ^{109}Sn and ^{111}Sn (causing radionuclide impurity through decay to ^{109}In and ^{111}In) are discussed. The numerical data of the measured cross sections are collected in Table 3-5. They are shown in graphical form in the corresponding sections discussing the different production routes.

4. Production routes

4.1. Indirect

The medically useful ^{110m}In is produced through the 100 % EC decay of ^{110}Sn . The production routes for ^{110}Sn include proton induced reactions at low and medium energy on stable isotopes of indium or alpha-particle and ^3He induced reactions on stable isotopes of cadmium.

4.1.1. In+p

The mother isotope ^{110}Sn can be obtained on the two stable isotopes of indium (^{113}In : 4.3 % and ^{115}In : 95.7 %), through the $^{113}\text{In}(p,4n)$ and $^{115}\text{In}(p,6n)$ reactions. As the high mass target isotope has an abundance of more than 95%, the (p,6n) reaction, needing incident energies of around 60 MeV, should be favorite for efficient production. From the point of view of radio-purity in any case, shorter-lived ^{111}Sn (decays to contaminating ^{111}In) and ^{113}Sn (decays to contaminating ^{113m}In) will be produced that will also have an influence on the specific activity of the final product. Presence of ^{111}Sn can be minimized by choosing the used energy range, irradiation time, or/and a proper cooling time before loading of the generator to let shorter-lived ^{111}Sn (and lower mass short-lived Sn radioisotopes) decay. Some contamination with $^{113m}\text{Sn} \rightarrow ^{113g}\text{Sn}$ can never be avoided but as high energy protons are needed

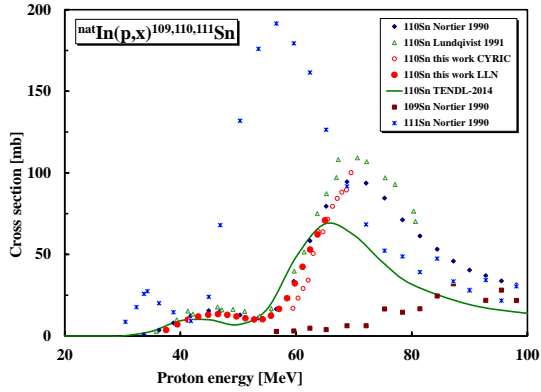
for the (p,4n) (threshold 28.8 MeV) and (p,6n) (threshold 44.8 MeV) reactions, limited target thickness will insure that the cross section for $^{113}\text{In}(p,n)$ in the target is low, as (p,n) reactions usually have maximum at much lower energies, so the protons leave the thin target before decelerating down into the energy range favorable for (p,n) reaction. Moreover, even if produced, the long half-life of ^{113g}Sn results in low activity of its decay product ^{113m}In and limited influence on the radio-purity. Radionuclides of Sn with mass lower than 110, and decaying to In radio-products, have even shorter half-life. Their presence could only be eliminated by keeping the incident proton energy below the threshold of the $^{113}\text{In}(p,5n)$ (threshold 40.2 MeV) reaction at the cost of large production losses. No experimental cross section data were found for activation cross sections on monoisotopic targets, only data on ^{nat}In were published. All available experimental activation cross section data for production of ^{109}Sn ($T_{1/2} = 18$ min), ^{110}Sn ($T_{1/2} = 4.167$ h) and ^{111}Sn ($T_{1/2} = 35.3$ min) are shown in Fig. 1. In our experiments we could deduce cross section data only for production of ^{110}Sn due to the long cooling time after EOB (end of bombardment). Two earlier data sets exist, measured by Lundquist et al. [24] and Nortier et al. [25, 26]. Our data for ^{110}Sn are in acceptable agreement with those. According to Fig. 1, no production of ^{109}Sn is observable up to 55 MeV, but the amount of ^{111}Sn is significant, resulting in high yield of the ^{111}In decay product. At energies above 60 MeV (the threshold of the $^{115}\text{In}(p,6n)^{110}\text{Sn}$ reaction is 44.8 MeV) the $^{111}\text{Sn}/^{110}\text{Sn}$ ratio is becoming better, therefore this energy range is preferred, resulting in high yields of ^{110m}In using targets with natural composition. The radionuclide purity can be improved significantly by using irradiation times up to 3 half-lives of ^{110}Sn and a longer cooling time to let the simultaneously produced shorter-lived ^{109}Sn and ^{111}Sn decay.

4.1.2. Cd+α

Another suggested route for the production of ^{110m}In through the $^{110}\text{Sn}/^{110m}\text{In}$ isotope generator is the $^{108}\text{Cd}(2n)^{110}\text{Sn}$ nuclear reaction [27] and at higher energies the $^{110}\text{Cd}(\alpha,4n)^{110}\text{Sn}$ reaction. We found only one relevant experimental data set, the production cross section of ^{110}Sn on ^{nat}Cd , published by us [9]. No data for ^{109}Sn and ^{111}Sn were given. The comparison of these experimental values and the theoretical data from TENDL-2014 is shown in Fig. 2. The TENDL-2014 prediction underestimates the magnitude but the shape is well reproduced. As ^{nat}Cd contains 8 stable isotopes (^{106}Cd -1.25 %, ^{108}Cd -0.89%, ^{110}Cd -12.49%, ^{111}Cd -12.80 %, ^{112}Cd -24.13 %, ^{113}Cd -12.22 %, ^{114}Cd -

Table 1: Main experimental parameters and methods of data evaluation

Reaction	Experiment				Data evaluation	
	$^{nat}\text{In}(p,x)$	$^{nat}\text{In}(p,x)$	$^{nat}\text{Ag}(\alpha,x)$	$^{nat}\text{Ag}(\alpha,\text{He},x)$		
Incident particle	Proton	Proton	α -particle	^3He	Gamma spectra evaluation	Genie 2000, Forgamma [12, 13]
Method	Stacked foil	Stacked foil	Stacked foil	Stacked foil	Determination of beam intensity	Faraday cup (preliminary)/Fitted monitor reaction (final) [14]
Target stack and thicknesses	Er(25 μm) Co(50 μm) Al(10 μm) In(50 μm) Al(100 μm) block Repeated 13 times	Al(11 μm) In(116.3 μm) Al(99.2 μm) V(8.41 μm) Al(99.2 μm) Ho(26.2 μm) Al(99.2 μm) block Repeated 19 times	2 stacks, each 8 Ag(8.1 μm) 6 Cu(7.4 μm)	17 Ag(8.1 μm) 3 Ti(12 μm)	Decay data	NUDAT 2.6 [15]
Number of target foils	13	19	16	17	Reaction Q-values	Q-value calculator [16]
Accelerator	K110 MeV cyclotron CYRIC, Sendai	K110 MeV cyclotron LLN Louvain-la-Neuve	CGR-560 cyclotron Brussels	MGC -20 cyclotron ATOMKI Debrecen	Determination of beam energy	Andersen and Ziegler (preliminary) [17] Fitted monitor reaction (final) [17]
Primary energy	70 MeV	65 MeV	27 MeV	26 MeV	Uncertainty of energy	Cumulative effects of possible uncertainties
Irradiation time	61 min	60 min	60 min	47 min	Cross sections	Isotopic cross section
Beam current	52 nA	50 nA	120 nA	101 nA	Uncertainty of cross sections	Sum in quadrature of all individual contribution [18]
Monitor reaction, [recommended values]	$^{27}\text{Al}(p,x)^{22,24}\text{Na}$ reaction [19]	$^{27}\text{Al}(p,x)^{22,24}\text{Na}$ reaction [19]	$^{nat}\text{Cu}(\alpha,x)^{66,67}\text{Ga}$ reaction [19]	$^{nat}\text{Ti}(\alpha,\text{He},x)^{48}\text{V}$ reaction [19]	Yield	Physical yield [20]
Monitor target and thickness	^{27}Al , 100 μm	^{27}Al , 99.2 μm	^{nat}Cu , 7.4 μm	^{nat}Ti , 12.7 μm	Theory	ALICE-IPPE [21], EMPIRE [22], TALYS (TENDL 2013, 2014) [23]
detector	HPGe	HPGe	HPGe	HPGe		
γ -spectra measurements	2 series	2 series	4 series	2 series		
Cooling times	22-30 h 315-340 h	8-12 h 141-193 h	0.3-2.5 h 5.1-8.3 h 22.1-48.9 h 52-99.7 h	0.5-3.7 h 3.9-11.8		


 Figure 1: Activation cross sections of proton induced nuclear reactions for $^{nat}\text{In}(p,x)^{109,110,111}\text{Sn}$

28.73 %, ^{116}Cd -7.49 %) many reactions of the (α, xn) type can contribute. When using ^{nat}Cd the contribution through the $^{106}\text{Cd}(\alpha, \gamma)$ reaction is very small. The lowest number of contaminating radioisotopes is obtained by relying on the $^{108}\text{Cd}(\alpha, 2n)^{110}\text{Sn}$ reaction as only shorter-lived ^{111}Sn will unavoidably be produced through the (α, n) reaction. Choosing an appropriate cooling time, allowing the decay of ^{111}Sn before preparing the generator, will result in practically nca (no carrier added) ^{110m}In . In principle we can also use ^{nat}Cd targets, because the additionally produced Sn isotopes are either stable or long-lived (^{113}Sn) and decay of this last results in negligible influence on the specific activity as discussed in the previous section. The highest yield and lowest contamination will be obtained by using highly enriched ^{108}Cd . No experimental data were presented on ^{108}Cd , but cross sections up to the threshold of $^{110}\text{Cd}(\alpha, 4n)^{110}\text{Sn}$ reaction (35.6 MeV) can be deduced from cross sections measured on ^{nat}Cd . The theoretical cross sections for production of $^{109,110,111}\text{Sn}$ by alpha irradiation of ^{nat}Cd are shown in Fig. 2. It can be seen on Fig. 3 and from Table 2 that using highly enriched ^{108}Cd targets, up to 30 MeV no contamination with ^{109}Sn exists. By using the 24-30 MeV energy range and the above mentioned long irradiation and longer cooling time also the amount of ^{111}Sn can be minimized.

4.1.3. $\text{Cd} + ^3\text{He}$

The situation is nearly the same as for the $\text{Cd} + \alpha$ route. The radionuclide of interest, ^{110}Sn , can also be

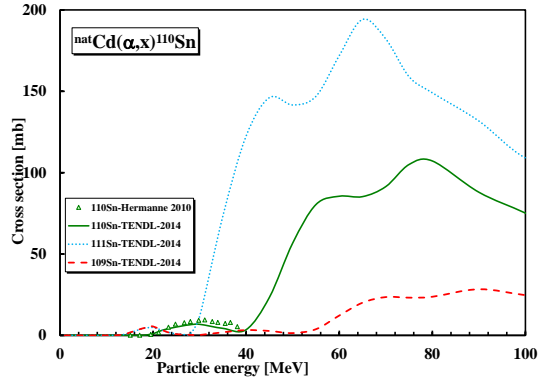


Figure 2: Excitation functions of the $^{nat}\text{Cd}(\alpha, xn)^{109,110,111}\text{Sn}$ reactions

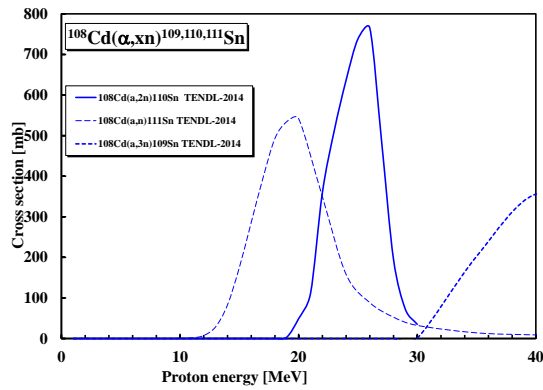


Figure 3: Theoretical excitation functions of the $^{108}\text{Cd}(\alpha, xn)^{109,110,111}\text{Sn}$ reactions

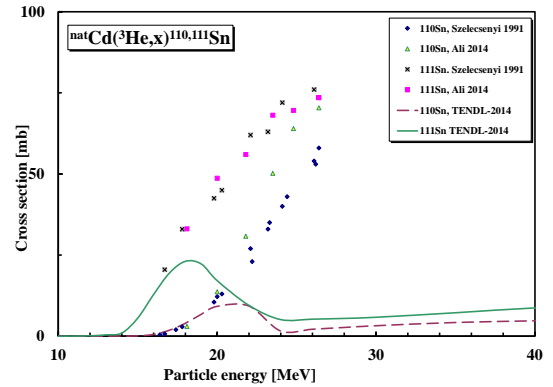


Figure 4: Excitation functions of the $^{nat}\text{Cd}({}^3\text{He}, xn)^{110,111}\text{Sn}$ reactions

produced through $^{nat}\text{Cd}({}^3\text{He}, xn)$ or, with higher yield, using enriched targets through the $^{110}\text{Cd}({}^3\text{He}, 3n)$ reaction. No experimental data exist for monoisotopic targets. Two earlier studies were published for production of ^{110}Sn and ^{111}Sn on ^{nat}Cd [2, 5] (reported by our group). The experimental data are shown in Fig. 4 in comparison with the TENDL-2014 calculation. A good agreement is seen between the two experimental datasets but the predictions of TENDL-2014 differ drastically, both in shape and in magnitude. The theoretical excitation functions of the $^{110}\text{Cd}({}^3\text{He}, xn)^{109,110,111}\text{Sn}$ reactions are shown in Fig. 5, but they are probably unrealistic as discussed above (according to the systematics on the neighboring elements the maximum cross sections of the $^{110}\text{Cd}({}^3\text{He}, 3n)$ reaction should be around 500-600 mb). When comparing the α and ${}^3\text{He}$ routes in the low energy region (up to 30 MeV) for the $^{108}\text{Cd}(\alpha, 2n)$ and the $^{110}\text{Cd}({}^3\text{He}, 3n)$ reactions, it can be seen that the cross sections on ^{108}Cd and ^{110}Cd are similar for the corresponding particles, therefore due to the lower stopping, the yield of the ${}^3\text{He}$ route should be higher. It is, however, well known that high intensity ${}^3\text{He}$ beams are rare and very expensive, even when a gas recovery system is available at the accelerator.

5. Direct production

The direct production routes include proton or deuteron induced reactions on cadmium and -particle or ${}^3\text{He}$ induced reactions on silver.

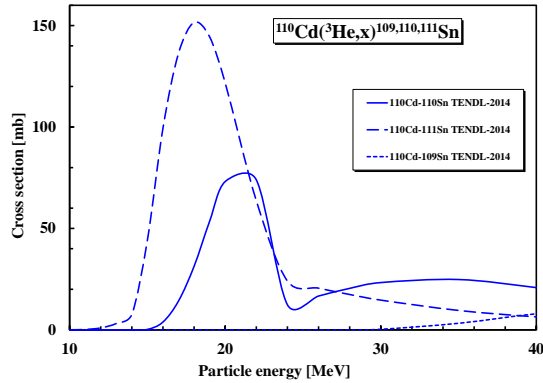


Figure 5: Theoretical excitation functions of the $^{110}\text{Cd}(^3\text{He},x)^{109,110,111}\text{Sn}$ reactions

5.1. Cd+p

Production of ^{110m}In ($T_{1/2} = 69.1$ min), with not too high contamination, via proton and deuteron induced reactions on Cd can only be done on highly enriched targets. When ^{nat}Cd is used, the many stable target isotopes lead to possible parallel production of various In radioisotopes with comparable or longer half-lives than ^{110m}In : ^{108m}In ($T_{1/2} = 39.6$ min), ^{108g}In ($T_{1/2} = 58$ min), ^{109}In ($T_{1/2} = 4.167$ h), ^{111}In ($T_{1/2} = 2.81$ d), ^{113m}In ($T_{1/2} = 99.48$ min), ^{114m}In ($T_{1/2} = 49.51$ d), ^{115m}In ($T_{1/2} = 4.436$ h), ^{116m}In ($T_{1/2} = 54.29$ min), ^{117}In ($T_{1/2} = 43.2$ min), ^{117m}In ($T_{1/2} = 1.937$ h). By irradiating highly enriched ^{110}Cd with protons in a limited energy range, only ^{110}In is produced through a (p,n) reaction. As it was mentioned before in a direct production route not only the metastable state ^{110m}In is produced, but also its longer-lived, higher spin ^{110g}In ground state ($T_{1/2} = 4.92$ h). The experimental and theoretical excitation functions for the $^{110}\text{Cd}(p,xn)^{110m,110g}\text{In}$ reactions are shown in Fig. 6 and 7. For ^{109}In production we present only the theoretical data in Fig. 7 to see the reaction threshold and the shape of the excitation function. Experimental data for the cross section of $^{110}\text{Cd}(p,n)^{110m}\text{In}$ reactions (Fig. 6) are available from Blaser et al. 1951 [28], Al Saleh et al. [29], Khandaker et al. [30], Trknyi et al. [3], Skakun et al. [31], Otozai et al. [32], Nortier et al. [25] and Kormali et al. [33]. The data measured on ^{nat}Cd were normalized for ^{110}Cd target up to the threshold of the $^{111}\text{Cd}(p,2n)^{110}\text{In}$ reaction. In Fig. 7 the excitation function of the $^{110}\text{Cd}(p,n)^{110g}\text{In}$ reaction is presented. Experimental data on ^{nat}Cd and ^{110}Cd are available from Skakun et al. [31], Abramovich et al. [34],

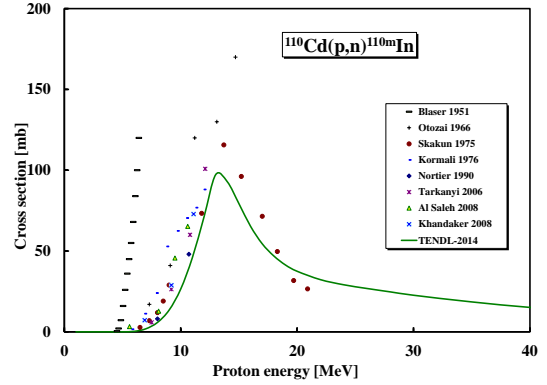


Figure 6: Excitation functions of the $^{110}\text{Cd}(p,n)^{110m}\text{In}$ reaction

Otozai et al. [32], Tarkanyi et al. [3] and Elbinawi et al. [35]. Fig. 7 shows that by properly selecting the incident energy, the contamination with ^{109}In can be minimized. Comparison of the Fig. 6 and Fig. 7 shows that the useful energy ranges for ^{110m}In and ^{110g}In production are the same. The cross sections for ^{110g}In are a factor of 6 higher and, in spite of the four times longer half-life, the activity ratio at EOB will still be unacceptable from the point of view of radionuclide purity. The ^{110m}In and ^{110g}In decay independently and the activity ratio during the irradiation will change in the target as the meta-state reaches saturation faster. Hence only rather short irradiations could help to reduce somewhat the contamination level.

5.2. Cd+d

As it was mentioned in the previous section on proton induced reactions on ^{nat}Cd , large amounts of different long-lived radioisotopes of indium are produced when using natural cadmium targets, hence the only realistic candidate is the $^{110}\text{Cd}(d,2n)$ reaction. Only a few measurements were published for the $^{110}\text{Cd}(d,2n)^{110m,110g}\text{In}$ reactions: Usher et al. 1977 [36], Mukhamedov et al. 1983 [37] and Tarkanyi et al. 2007 [4]. The excitation functions are shown in Figs. 8-9. In Fig. 8 the theoretical excitation functions for production of ^{109}In and ^{111}In are also shown to illustrate the shape and the magnitude of these simultaneously produced neighboring indium radioisotopes. According to Figs. 8-9 a very narrow energy window around 15 MeV exists, where the ^{110m}In yield is high and the co-produced ^{109}In and ^{111}In amounts are the lowest. A significant impurity of

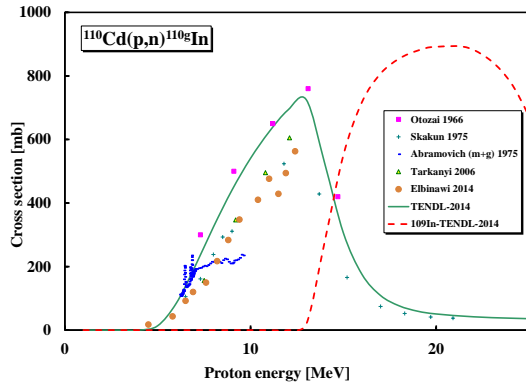


Figure 7: Excitation functions of the $^{110}\text{Cd}(p,n)^{110g}\text{In}$ and $^{110}\text{Cd}(p,n)^{109}\text{In}$ reactions

^{110g}In , practically independently from the covered energy range, will however be co-produced as the values of the cross sections are about the same.

5.3. Ag+ α

Other possible target particle combinations for direct production of ^{110m}In are the Ag+ α and Ag+ ^3He reactions. Silver has two stable isotopes: ^{107}Ag (abundance 51.839 %) and ^{109}Ag (48.161 %). When considering alpha induced reactions, the $^{107}\text{Ag}(\alpha,n)$ is the main candidate as it allows to minimize co-produced contaminants. Cross sections for direct production of $^{110m,g}\text{In}$ through alpha induced nuclear reactions on silver have been measured by Miselides et al. [38], Chaubey et al. [39], Fukushima et al. [40], Takacs et al. [7] (our work), Wasilewsky et al. [41], Omori et al. [42], Singh et al. [43] and in the present work. The excitation functions of the $^{107}\text{Ag}(\alpha,xn)^{110m}\text{In}$, ^{109}In , ^{110g}In reactions are shown in Fig 10-12. According to Fig. 12 the production of ^{109}In is starting only above 16 MeV. The impurity from the ground state ^{110g}In is high over the whole energy range. From literature it is well known that when ^{nat}Cd targets are used, longer-lived reaction products are present practically in the whole energy range. Especially for the medically important ^{111}In , most frequently produced though the $^{112}\text{Cd}(p,2n)$ reaction with 24-25 MeV incident proton energy, the $^{109}\text{Ag}(\alpha,2n)$ could be a real alternative production route, taking into account that the ^{111}In can be produced with high yields and low impurity levels. A large number of measurements were done for the $^{109}\text{Ag}(\alpha,2n)^{111}\text{In}$ reaction: Patel et al. [44] Hasbroek et al. [45], Ismail et al. [46], Wasilewsky et

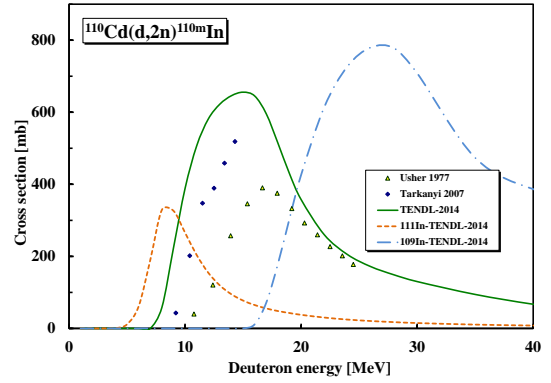


Figure 8: Excitation functions of the $^{110}\text{Cd}(d,xn)^{109,110m,111}\text{In}$ reactions

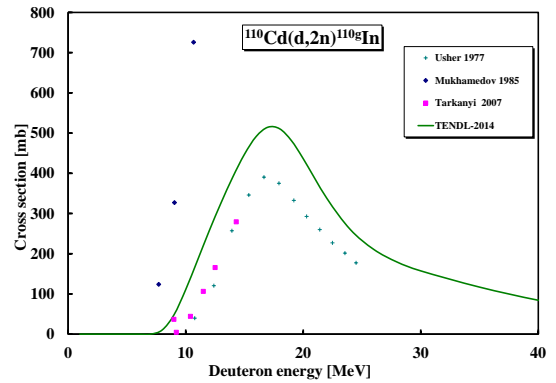


Figure 9: Excitation functions of the $^{110}\text{Cd}(d,2n)^{110g}\text{In}$ nuclear reaction

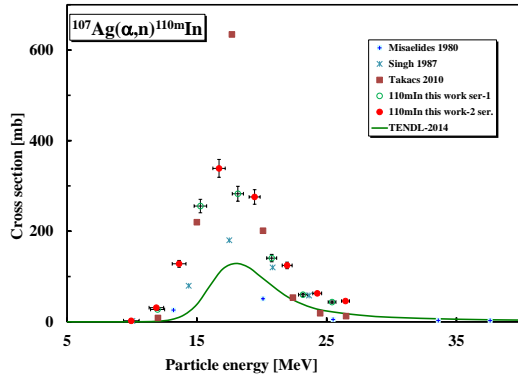


Figure 10: Excitation functions of the $^{107}\text{Ag}(\alpha,n)^{110m}\text{In}$ nuclear reaction

al. [47], Takacs et al. [7], Mukherjee et al. [48], Guin et al. [49], Chaubey [39], Fukushima [40], Chuvilskaya [50], Peng [51], Bleuer [52], Porges [53], Xiufeng [54], Singh et al. [43] and the present work. The experimental results are shown in Fig. 13.

5.4. $\text{Ag}+^3\text{He}$

When using ^3He beams the useful reaction on Ag is $^{109}\text{Ag}(^3\text{He},2n)$. The disturbing products are ^{109}In , ^{110g}In and ^{111}In . The excitation functions for $^{109}\text{Ag}(^3\text{He},xn)^{109,110m,110g,111}\text{In}$ are shown in Figs 14-17. The low reliability of predictions of TENDL-2014 for ^3He induced processes can be remarked for these four reactions. The experimental cross section data on the $^{109}\text{Ag}(^3\text{He},2n)^{110m,g}\text{In}$ reactions were measured by Misaelides et al. [38], Marten et al. [55], Nagame et al. [56], Omori et al. [57] and in this work. According to Fig. 14, the cross sections for production of ^{110m}In are low. The reaction can effectively be used in the 10-30 MeV range but over the whole energy range a significant yield for ^{109}In is seen (Fig. 17). Small cross sections for ^{111}In production are also present over the whole energy range (Fig. 16) and for ^{110g}In the cross sections are similar to those for ^{110m}In (Fig. 15).

6. Integral yields

Integral yields as a function of energy were calculated by using fitted experimental and/or theoretical cross sections for production of ^{110}Sn via the $^{113}\text{In}(p,4n)$, $^{nat}\text{In}(p,xn)$, $^{108}\text{Cd}(\alpha,2n)$, $^{nat}\text{Cd}(\alpha,xn)$, $^{110}\text{Cd}(^3\text{He},3n)$ and $^{nat}\text{Cd}(^3\text{He},xn)$ reactions and for direct production

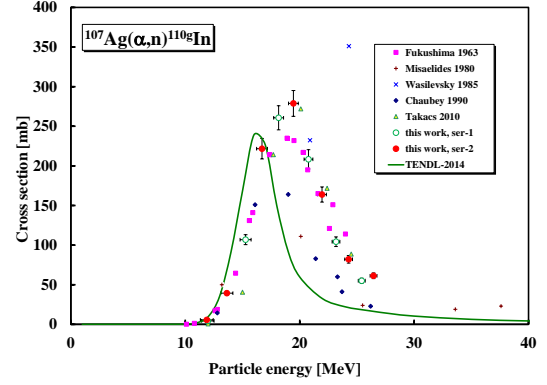


Figure 11: Excitation functions of the $^{107}\text{Ag}(\alpha,n)^{110g}\text{In}$ nuclear reaction

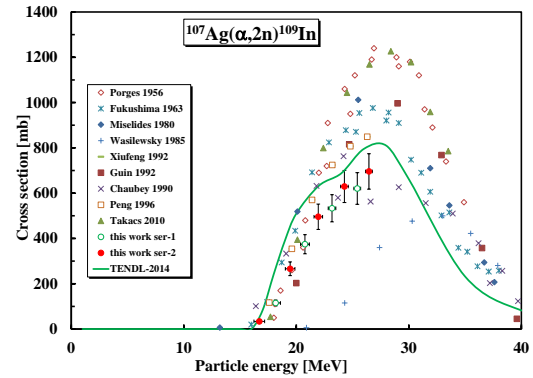


Figure 12: Excitation functions of the $^{107}\text{Ag}(\alpha,2n)^{109}\text{In}$ nuclear reaction

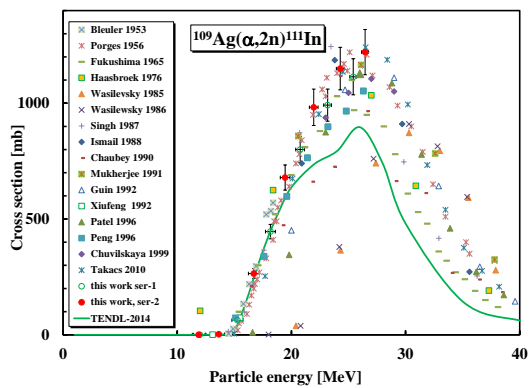


Figure 13: Excitation functions of the $^{109}\text{Ag}(\alpha,2n)^{111}\text{In}$ nuclear reaction

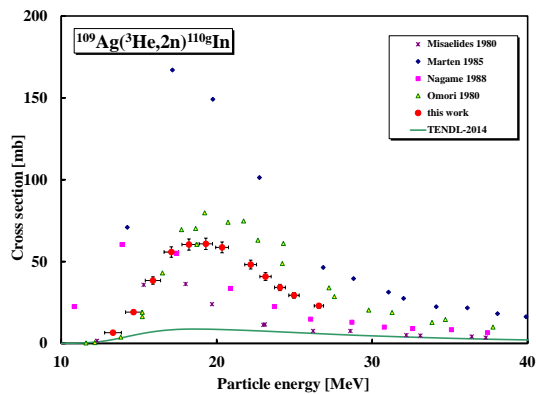


Figure 15: Excitation functions of the $^{109}\text{Ag}({}^3\text{He},2n)^{110g}\text{In}$ nuclear reaction

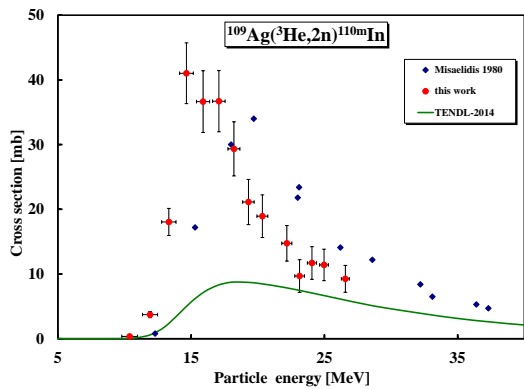


Figure 14: Excitation functions of the $^{109}\text{Ag}({}^3\text{He},xn)^{110m}\text{In}$ nuclear reaction

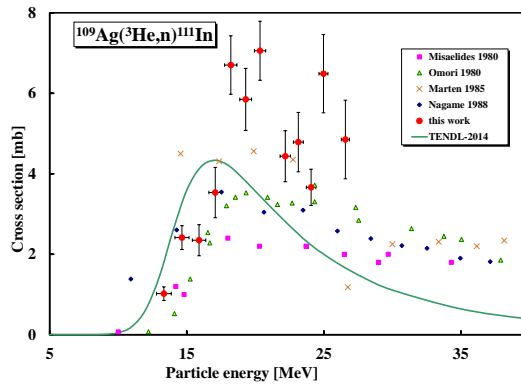


Figure 16: Excitation functions of the $^{109}\text{Ag}({}^3\text{He},n)^{111}\text{In}$ nuclear reaction

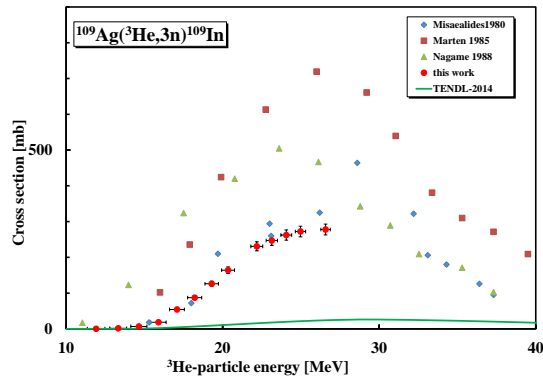


Figure 17: Excitation functions of the $^{109}\text{Ag}(^3\text{He},3\text{n})^{109}\text{In}$ nuclear reaction

of $^{110\text{m}}\text{In}$ via $^{110}\text{Cd}(\text{p},\text{n})$, $^{110}\text{Cd}(\text{d},2\text{n})$, $^{107}\text{Ag}(\alpha,\text{xn})$ and $^{109}\text{Ag}(^3\text{He},2\text{n})$ reactions (Figs. 18-19). There are only a few experimental thick target yields on these target-reaction combinations measured by Dmitriev [58, 59], Nickles et al. [60], Mukhamedov [37] and Abe et al. [61]. Where an energy overlap is existing, our data were compared with those literature values.

7. Summary

In the frame of a systematic study of production routes of the medically useful $^{110\text{m}}\text{In}$, experimental cross section data for the $^{nat}\text{In}(\text{p},\text{xn})^{110}\text{Sn}$ indirect route and for $^{nat}\text{Ag}(\alpha,\text{xn})^{109,110\text{m},110\text{g},111}\text{In}$ and $^{nat}\text{Ag}(^3\text{He},\text{xn})^{109,110\text{m},110\text{g},111}\text{In}$ direct nuclear reactions were measured. The new data are in good agreement with earlier results and are in acceptable agreement with the theoretical predictions in TENDL-2014 except for the ^3He induced reactions. Thick target yields were derived for different routes relevant for production of the radioisotope of interest $^{110\text{m}}\text{In}$. The $^{110}\text{Sn}(^{110\text{m}}\text{In})$ generator could be prepared at low and medium energies with light charged particles via the $^{113}\text{In}(\text{p},4\text{n})$, $^{nat}\text{In}(\text{p},\text{xn})$, $^{110}\text{Cd}(\alpha,2\text{n})$, $^{nat}\text{Cd}(\alpha,\text{xn})$, $^{110}\text{Cd}(^3\text{He},3\text{n})$ and $^{nat}\text{Cd}(^3\text{He},\text{xn})$ reactions. Each of these routes requires high incident energy and a proper selection of an adapted energy range. The main advantage of the indirect method is the high radionuclide purity, which can easily be assured by the proper irradiation and cooling parameters. Another advantage is that, depending on the required specific activity, natural targets can be used. Considering the available commercial accelera-

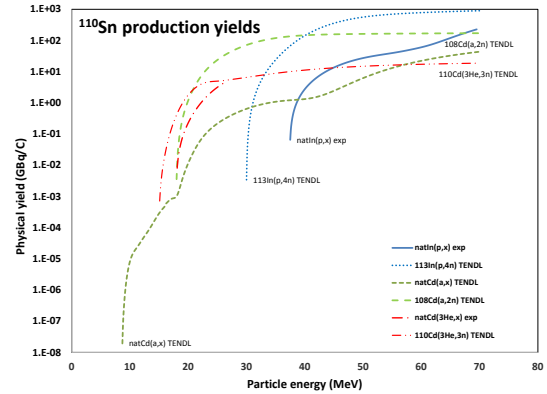


Figure 18: Thick target yields for production of ^{110}Sn

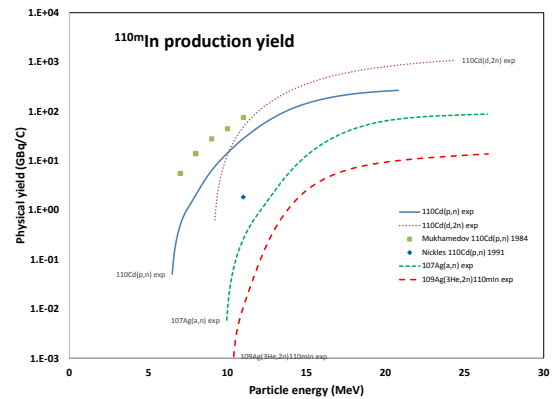


Figure 19: Thick target yields for production of $^{110\text{m}}\text{In}$

tors, use of the $^{nat}\text{In}(p,xn)^{110}\text{Sn}$ reaction seems to be the simplest and most productive method, however requiring 70-100 MeV beam energy. It should be mentioned that the generator can be produced also at lower energy machines by using 30 MeV alpha beams and enriched ^{108}Cd targets. For direct production the $^{110}\text{Cd}(p,n)$, $^{110}\text{Cd}(d,2n)$, $^{107}\text{Ag}(\alpha,xn)$ and $^{109}\text{Ag}(^3\text{He},2n)$ reactions are the most suitable candidate routes. Lower energy accelerators can also be used, but highly enriched targets are required. Although the radionuclide impurity level is lower, significant amount of ^{110g}In are always present in the product. If the ^{110g}In level is not taken into account, the $^{110}\text{Cd}(p,n)$ reaction seems the most promising production route.

8. Acknowledgements

This work was performed in the frame of the HAS-FWO Vlaanderen (Hungary-Belgium) project. The authors acknowledge the support of the research project and of the respective institutions (CYRIC, VUB, LLN) in providing the beam time and experimental facilities.

References

- [1] A. L. Nichols, R. Capote Noy, Summary report, first research coordination meeting on nuclear data for charged-particle monitor reactions and medical isotope production, Tech. rep., IAEA (2013).
- [2] F. Szelecsényi, Z. Kovács, F. Tárkányi, G. Tóth, Production of ^{110}In for PET investigation via $\text{Cd}(3\text{He},xn)^{110}\text{Sn}$ - ^{110}In reaction with low energy cyclotron, *Journal of Labelled Compounds and Radiopharmaceuticals* 30 (1991) 98–99.
- [3] F. Tárkányi, B. Király, F. Ditrói, S. Takács, J. Csikai, A. Hermanne, M. S. Uddin, M. Hagiwara, A. Baba, T. Ido, Y. N. Shubin, S. F. Kovalev, Activation cross-sections on cadmium: Proton induced nuclear reactions up to 80 MeV, *Nuclear Instruments & Methods in Physics Research Section B* 245 (2) (2006) 379–394.
- [4] F. Tárkányi, B. Király, F. Ditrói, S. Takács, J. Csikai, A. Hermanne, M. S. Uddin, M. Hagiwara, M. Baba, T. Ido, Y. N. Shubin, S. F. Kovalev, Activation cross sections on cadmium: Deuteron induced nuclear reactions up to 40 MeV, *Nuclear Instruments & Methods in Physics Research Section B* 259 (2) (2007) 817–828.
- [5] B. M. Ali, M. Al-Abyad, U. Seddik, S. U. El-Kameesy, F. Ditrói, S. Takács, F. Tárkányi, Experimental investigation and theoretical calculation of he-3-particle induced nuclear reactions on cadmium up to 27 MeV, *Nuclear Instruments & Methods in Physics Research Section B* 321 (2014) 30–40.
- [6] F. Tárkányi, S. Takács, A. Hermanne, P. Van den Winkel, R. Van der Zwart, Y. A. Skakun, Y. N. Shubin, S. F. Kovalev, Investigation of the production of the therapeutic radioisotope ^{114m}In through proton and deuteron induced nuclear reactions on cadmium, *Radiochimica Acta* 93 (9-10) (2005) 561–569.
- [7] S. Takács, A. Hermanne, F. Tárkányi, A. Ignatyuk, Cross-sections for alpha particle produced radionuclides on natural silver, *Nuclear Instruments & Methods in Physics Research Section B* 268 (1) (2010) 2–12.
- [8] F. Tárkányi, A. Hermanne, B. Király, S. Takács, F. Ditrói, M. Baba, A. V. Ignatyuk, Investigation of activation cross sections of deuteron induced reactions on indium up to 40 MeV for production of a $\text{Sn-113}/\text{In-113m}$ generator, *Applied Radiation and Isotopes* 69 (1) (2011) 26–36.
- [9] A. Hermanne, L. Daraban, R. A. Rebeles, A. Ignatyuk, F. Tárkányi, S. Takács, Alpha induced reactions on natCd up to 38.5 MeV: Experimental and theoretical studies of the excitation functions, *Nuclear Instruments & Methods in Physics Research Section B* 268 (9) (2010) 1376–1391.
- [10] S. Takács, F. Tárkányi, A. Hermanne, R. A. Rebeles, Activation cross sections of proton induced nuclear reactions on natural hafnium, *Nuclear Instruments & Methods in Physics Research Section B-Beam Interactions with Materials and Atoms* 269 (23) (2011) 2824–2834.
- [11] F. Tárkányi, F. Ditrói, S. Takács, B. Király, A. Hermanne, M. Sonck, M. Baba, A. V. Ignatyuk, Investigation of activation cross-sections of deuteron induced nuclear reactions on natMo up to 50 MeV, *Nuclear Instruments & Methods in Physics Research Section B-Beam Interactions with Materials and Atoms* 274 (2012) 1–25.
- [12] Canberra, http://www.canberra.com/products/radiochemistry_lab/genie-2000-software.asp. (2000).
- [13] G. Székely, Fgm - a flexible gamma-spectrum analysis program for a small computer, *Computer Physics Communications* 34 (3) (1985) 313–324.
- [14] F. Tárkányi, F. Szelecsényi, S. Takács, Determination of effective bombarding energies and fluxes using improved stacked-foil technique, *Acta Radiologica, Supplementum* 376 (1991) 72.
- [15] R. R. Kinsey, C. L. Dunford, J. K. Tuli, T. W. Burrows, in *Capture Gamma Ray Spectroscopy and Related Topics*, Vol. 2. (NUDAT 2.6 <http://www.nndc.bnl.gov/nudat2/>), Vol. 2, Springer Hungarica Ltd, Budapest, 1997.
- [16] B. Pritychenko, A. Sonzogni, Q-value calculator (2003).
- [17] H. H. Andersen, J. F. Ziegler, Hydrogen stopping powers and ranges in all elements. The stopping and ranges of ions in matter, Volume 3., *The Stopping and ranges of ions in matter*, Pergamon Press, New York, 1977.
- [18] International-Bureau-of-Weights-and-Measures, Guide to the expression of uncertainty in measurement, 1st Edition, International Organization for Standardization, Genève, Switzerland, 1993.
- [19] F. Tárkányi, S. Takács, K. Gul, A. Hermanne, M. G. Mustafa, M. Nortier, P. Oblozinsky, S. M. Qaim, B. Scholten, Y. N. Shubin, Z. Youxiang, TECDOC 1211, IAEA, beam monitor reactions (chapter 4). charged particle cross-section database for medical radioisotope production: diagnostic radioisotopes and monitor reactions., Tech. rep., IAEA (2001).
- [20] M. Bonardi, The contribution to nuclear data for biomedical radioisotope production from the milan cyclotron facility (1987).
- [21] A. I. Dityuk, A. Y. Konobeyev, V. P. Lunev, Y. N. Shubin, New version of the advanced computer code ALICE-IPPE, Tech. rep., IAEA (1998).
- [22] M. Herman, R. Capote, B. V. Carlson, P. Oblozinsky, M. Sin, A. Trkov, H. Wienke, V. Zerkin, Empire: Nuclear reaction model code system for data evaluation, *Nuclear Data Sheets* 108 (12) (2007) 2655–2715.
- [23] A. J. Koning, D. Rochman, Modern nuclear data evaluation with the TALYS code system, *Nuclear Data Sheets* 113 (2012) 2841.
- [24] H. Lundqvist, S. Scottrobson, L. Einarsson, P. Malmberg, Sn-110 In-110 - a new generator system for positron emission tomography, *Applied Radiation and Isotopes* 42 (5) (1991) 447–450.
- [25] F. M. Nortier, S. J. Mills, G. F. Steyn, Excitation-functions and production-rates of relevance to the production of ^{111}In by

- proton-bombardment of natCd and natIn up to 100 MeV, Applied Radiation and Isotopes 41 (12) (1990) 1201–1208.
- [26] F. M. Nortier, S. J. Mills, G. F. Steyn, Excitation-functions for the production of Cd-109, In-109 and Sn-109 in proton-bombardment of indium up to 200 MeV, Applied Radiation and Isotopes 42 (11) (1991) 1105–1107.
- [27] H. Thisgaard, M. Jensen, H. J. Jensen, The 108Cd(α ,n)110Sn nuclear reaction a production route to the PET radionuclide 110mIn (2004).
- [28] J. P. Blaser, F. Boehm, P. Marmier, D. C. Peaslee, Fonctions d'excitation de la reaction (p,n), i, Helvetica Physica Acta 24 (1951) 3.
- [29] F. S. Al-Saleh, Cross sections of proton induced nuclear reactions on natural cadmium leading to the formation of radionuclides of indium, Radiochimica Acta 96 (8) (2008) 461–465.
- [30] M. U. Khandaker, K. Kim, M. W. Lee, K. S. Kim, G. N. Kim, Y. S. Cho, Y. O. Lee, Production cross-sections for the residual radionuclides from the (nat)Cd(p, x) nuclear processes, Nuclear Instruments & Methods in Physics Research Section B-Beam Interactions with Materials and Atoms 266 (22) (2008) 4877–4887.
- [31] E. A. Skakun, A. P. Klyucharev, Y. N. Rakivnenko, I. A. Romani, Relative cross-sections for formation of indium isomers in (pn)-reaction and (p,2n)-reaction on cadmium isotopes, Izvestiya Akademii Nauk Sssr Seriya Fizicheskaya 39 (1) (1975) 31–36.
- [32] K. Otozai, S. Kume, A. Mito, H. Okamura, R. Tsujino, Excitation functions for the reactions induced by protons on cd up to 37 MeV, Nuclear Physics 80 (1966) 335–348.
- [33] S. M. Kormali, D. L. Swindle, E. A. Schweikert, Charged-particle activation of medium Z-elements. 2. proton excitation-functions, Journal of Radioanalytical Chemistry 31 (2) (1976) 437–450.
- [34] S. N. Abramovich, B. Y. Guzhovskii, A. G. Zvenigorodskii, S. V. Trusillo, Isobar-analog resonances, appearing in elastic proton-scattering and (pn)-reaction on 110, 112, 114, Cd-116 nuclei, Izvestiya Akademii Nauk Sssr Seriya Fizicheskaya 39 (8) (1975) 1688–1694.
- [35] A. Elbinawi, M. Al-Abyad, A. Sayed, M. I. El-Zaiki, U. Seddik, K. E. Abd-Elmageed, Integral radionuclide activation yield and evaluated cross section data for proton induced reactions with Cd for practical applications, Arab Journal of Nuclear Science and Applications 47 (3) (2014) 104–116.
- [36] O. H. Usher, E. Maceiras, M. C. Saravi, S. J. Nassiff, Production cross-sections and isomeric ratios for isomeric pair in-110m-in-110g Formed in Cd (d,xn) reactions, Radiochimica Acta 24 (2-3) (1977) 55–57.
- [37] S. Mukhammedov, A. Vasidov, E. Pardaev, Use of proton and deuteron activation methods of analysis in the determination of elements with Z \leq 42, Soviet Atomic Energy 56 (1) (1984) 56–58.
- [38] P. Misaelides, H. Munzel, Excitation-functions for He-3-induced and alpha-induced reactions with Ag-107 and Ag-109, Journal of Inorganic & Nuclear Chemistry 42 (7) (1980) 937–948.
- [39] A. K. Chaubey, M. K. Bhardwaj, R. P. Gautam, R. K. Y. Singh, M. A. Ansari, I. A. Rizvi, H. Singh, Preequilibrium decay process in the alpha induced reactions of silver isotopes, Applied Radiation and Isotopes 41 (4) (1990) 401–405.
- [40] S. Fukushima, S. Hayashi, S. Kume, H. Okamura, K. Otozai, K. Sakamoto, Y. Yoshizawa, Excitation functions for the reactions induced by alpha particles on 107Ag, Nuclear Physics 41 (1963) 275–197.
- [41] C. Wasilevsky, M. D. Vedoya, S. J. Nassiff, Excitation-functions for (alpha,xn) reactions on Ag-107 and Ag-109, Journal of Radioanalytical and Nuclear Chemistry 89 (2) (1985) 531–543.
- [42] T. Omori, K. Omori, C. Ochi, K. Yoshihara, M. Yagi, Simultaneous production of Tc-96 and In-111 by alpha-particle irradiation of stacked Nb and Ag foils, and their carrier-free separations, Journal of Radioanalytical and Nuclear Chemistry 82 (1) (1984) 61–69.
- [43] N. L. Singh, S. Agarwal, L. Chaturvedi, J. R. Rao, Excitation-functions for radioactive isotopes produced by alpha-particle induced reactions with silver, Nuclear Instruments & Methods in Physics Research Section B-Beam Interactions with Materials and Atoms 24-5 (1987) 480–483.
- [44] H. B. Patel, M. S. Gadkari, B. Dave, N. L. Singh, S. Mukherjee, Analysis of the excitation function of alpha-particle-induced reactions on natural silver, Canadian Journal of Physics 74 (9-10) (1996) 618–625.
- [45] F. J. Haasbroek, G. F. Burdzik, M. Cogneau, P. Wanet, Excitation functions and thick-target yields for 67Ga, 68Ge/68Ga, 109Cd and 111In induced in natural zinc and silver by 100 MeV alpha particles, Tech. rep., Council of Scientific and Industrial Research (1976).
- [46] M. Ismail, A. S. Divata, Measurement, analysis of alpha-induced reactions on Ta, Ag, Co, Pramana-J. Phys. 30 (1988) 193–210.
- [47] C. Wasilevsky, M. D. Vedoya, S. J. Nassiff, Cross-sections and isomeric ratios for the Ag-109(Alpha,N)in-112m,G and Ag-109(Alpha,2n)in-111m,G reactions, Applied Radiation and Isotopes 37 (4) (1986) 319–322.
- [48] S. Mukherjee, A. V. M. Rao, J. R. Rao, Preequilibrium analysis of the excitation-functions of (alpha,xn) reactions on silver and holmium, Nuovo Cimento Della Societa Italiana Di Fisica a-Nuclei Particles and Fields 104 (6) (1991) 863–874.
- [49] R. Guin, S. K. Saha, S. Prakash, M. Uhl, Isomeric yield ratios and excitation-functions in alpha-induced reactions on Ag-107, Ag-109, Physical Review C 46 (1) (1992) 250–257.
- [50] T. V. Chuvilskaya, Y. G. Seleznev, A. A. Shirokova, M. Herman, Yields of isomers from the reactions 107,109Ag(4He,xn), 41K(α ,n), and 193Ir(α ,n), Bull. Russ. Acad. Sci. Phys. (translation) 63 (1999) 825.
- [51] X. F. Peng, X. G. Long, F. Q. He, M. T. Liu, Excitation functions and yields of the reactions induced by alpha-particle bombardment of natural silver, Applied Radiation and Isotopes 47 (3) (1996) 309–313.
- [52] E. Bleuler, A. K. Stebbins, D. J. Tendam, The (α ,n) and (α ,2n) cross sections of 109Ag, Phys. Rev. 90 (1953) 460–463.
- [53] K. G. Porges, Alpha excitation functions of silver and copper, Phys. Rev. 101 (1956) 225–230.
- [54] P. Xiufeng, L. Mantian, H. Fuqing, L. Xianguan, Excitation functions for the Ag-107(α ,n)In-110-m,Ag-107(α ,2n)In-109 and Ag-109(α ,2n)In-111 reactions, Tech. rep. (1992).
- [55] M. Marten, A. Schuring, W. Scobel, H. J. Probst, Preequilibrium neutron emission in Ag-109(He-3,Xn) and Cd-111(P,Xn) reactions, Zeitschrift Fur Physik a-Hadrons and Nuclei 322 (1) (1985) 93–103.
- [56] Y. Nagame, Y. Nakamura, M. Takahashi, K. Sueki, H. Nakahara, Pre-equilibrium process in He-3-induced reactions on Co-59, Ag-109, Ta-181 and Bi-209, Nuclear Physics A 486 (1) (1988) 77–90.
- [57] T. Omori, M. Yagi, H. Yamazaki, T. Shiokawa, Excitation-functions for He-3-induced reactions on silver, Radiochemical and Radioanalytical Letters 44 (5) (1980) 307–314.
- [58] P. P. Dmitriev, Radionuclide yield in reactions with protons, deuterons, alpha particles and helium-3, Tech. rep., IAEA (1986).
- [59] P. P. Dmitriev, Systematics of nuclear reaction yields for thick target at 22 MeV proton energy, Vop. At. Nauki i Tekhn., Ser.Yadernye Konstanty 57 (1983) 2.

- [60] R. J. Nickles, A shotgun approach to the chart of the nuclides. radiotracer production with an 11 MeV proton cyclotron, *Acta Radiologica, Supplementum* 376 (1991) 69–71.
- [61] K. Abe, A. Iizuka, A. Hasegawa, S. Morozumi, Induced radioactivity of component materials by 16-MeV protons and 30-MeV alpha-particles, *Journal of Nuclear Materials* 123 (1-3) (1984) 972–976.

Table 2: Decay characteristics of the investigated reaction products and Q-values of reactions for their productions

Nuclide Decay mode Level energy	Half-life	E _γ (keV)	I _γ (%)	Contributing reaction	Q-value(keV)
¹⁰⁹ In β ⁺ : 6.6 % EC: 93.4 %	4.167 h	331.2 649.8 1099.2 1321.3	9.7 28 30 11.9	¹⁰⁷ Ag(³ He,n) ¹⁰⁹ Ag(³ He,3n) ¹⁰⁷ Ag(α,2n) ¹⁰⁹ Ag(α,4n) ¹¹⁰ Cd(p,2n) ¹¹¹ Cd(p,3n) ¹¹² Cd(p,4n) ¹¹³ Cd(p,5n) ¹¹⁴ Cd(p,6n) ¹¹⁶ Cd(p,8n) ¹⁰⁸ Cd(d,n) ¹¹⁰ Cd(d,3n) ¹¹¹ Cd(d,4n) ¹¹² Cd(d,5n) ¹¹³ Cd(d,6n) ¹¹⁴ Cd(d,7n) ¹¹⁶ Cd(d,9n)	4941.24 -11514.7 -15636.39 -32092.32 -12714.5 -19690.14 -29084.19 -35622.95 -44665.87 -59506.21 2299.78 -14939.08 -21914.71 -31308.76 -37847.52 -46890.43 -61730.77
^{110m} In β ⁺ : 61.25 %EC: 38.75 % 62.084 keV	69.1 min	657.75 818.05 1125.77	97.74 0.87 1.04	¹⁰⁹ Ag(³ He,2n) ¹⁰⁷ Ag(α,n) ¹⁰⁹ Ag(α,3n) ¹¹⁰ Cd(p,n) ¹¹¹ Cd(p,2n) ¹¹² Cd(p,3n) ¹¹³ Cd(p,4n) ¹¹⁴ Cd(p,5n) ¹¹⁶ Cd(p,7n) ¹¹⁰ Cd(d,2n) ¹¹¹ Cd(d,3n) ¹¹² Cd(d,4n) ¹¹³ Cd(d,5n) ¹¹⁴ Cd(d,6n) ¹¹⁶ Cd(d,8n)	-3460.5 -7582.2 -24038.2 -4660.3 -11636.0 -21030.0 -27568.8 -36611.7 -51452.1 -6884.9 -13860.6 -23254.6 -29793.4 -38836.3 -53676.6
^{110g} In β ⁺ : 0.008 %EC: 99.992 %	4.92 h	641.68 657.750 707.40 884.667 937.478 997.16	26.098 29.5 93 68.4 10.5	¹⁰⁹ Ag(³ He,2n) ¹⁰⁷ Ag(α,n) ¹⁰⁹ Ag(α,3n) ¹¹⁰ Cd(p,n) ¹¹¹ Cd(p,2n) ¹¹² Cd(p,3n) ¹¹³ Cd(p,4n) ¹¹⁴ Cd(p,5n) ¹¹⁶ Cd(p,7n) ¹¹⁰ Cd(d,2n) ¹¹¹ Cd(d,3n) ¹¹² Cd(d,4n) ¹¹³ Cd(d,5n) ¹¹⁴ Cd(d,6n) ¹¹⁶ Cd(d,8n)	-3460.5 -7582.2 -24038.2 -4660.3 -11636.0 -21030.0 -27568.8 -36611.7 -51452.1 -6884.9 -13860.6 -23254.6 -29793.4 -38836.3 -53676.6
¹¹¹ In EC: 100 %	2.81 d	171.28 245.35	90.7 94.1	¹⁰⁹ Ag(³ He,n) ¹⁰⁹ Ag(α,2n) ¹¹¹ Cd(p,n) ¹¹² Cd(p,2n) ¹¹³ Cd(p,3n) ¹¹⁴ Cd(p,4n) ¹¹⁶ Cd(p,6n) ¹¹⁰ Cd(d,n) ¹¹¹ Cd(d,2n) ¹¹² Cd(d,3n) ¹¹³ Cd(d,4n) ¹¹⁴ Cd(d,5n) ¹¹⁶ Cd(d,7n)	6530.92 -14046.71 -19690.14 -11038.57 -17577.34 -26620.26 -41460.61 3106.54 -3869.1 -13263.15 -19801.91 -28844.83 -43685.18
¹⁰⁹ Sn β ⁺ :6.6 % EC: 83.4 %	18.0 min	649.8 1099.2 1321.3	28 30 11.9	¹¹³ In(p,5n) ¹¹³ In(p,7n) ¹⁰⁸ Cd(³ He,2n) ¹¹⁰ Cd(³ He,4n) ¹¹¹ Cd(³ He,5n) ¹¹² Cd(³ He,6n) ¹¹³ Cd(³ He,7n) ¹¹⁴ Cd(³ He,8n) ¹⁰⁶ Cd(α,n) ¹⁰⁸ Cd(α,3n) ¹¹⁰ Cd(α,5n) ¹¹¹ Cd(α,6n) ¹¹² Cd(α,7n) ¹¹³ Cd(α,8n) ¹¹⁴ Cd(α,10n)	-39802.54 -56115.7 -7833.06 -25071.91 -32047.55 -41441.59 -47980.36 -57023.26 -10147.5 -28410.69 -45649.54 -52625.16 -62019.21 -68557.96

Table 2: continued

^{110}Sn EC: 100 %	4.167 h	280.462	97	$^{108}\text{Cd}(^3\text{He},n)$ $^{110}\text{Cd}(^3\text{He},3n)$ $^{111}\text{Cd}(^3\text{He},4n)$ $^{112}\text{Cd}(^3\text{He},5n)$ $^{113}\text{Cd}(^3\text{He},6n)$ $^{114}\text{Cd}(^3\text{He},7n)$ $^{116}\text{Cd}(^3\text{He},9n)$ $^{108}\text{Cd}(\alpha,2n)$ $^{110}\text{Cd}(\alpha,4n)$ $^{111}\text{Cd}(\alpha,5n)$ $^{112}\text{Cd}(\alpha,6n)$ $^{113}\text{Cd}(\alpha,7n)$ $^{114}\text{Cd}(\alpha,8n)$ $^{113}\text{In}(p,4n)$ $^{115}\text{In}(p,6n)$	3449.3 -13789.5 -20765.2 -30159.2 -36698.0 -45740.9 -60581.2 -17128.3 -34367.1 -41342.8 -50736.8 -57275.6 -66318.5 -28520.1 -44833.3
^{111}Sn β^+ : 30.2009 % EC: 69.7991 %	35.3 min	761.971152.98	1.482.7	$^{110}\text{Cd}(^3\text{He},2n)$ $^{111}\text{Cd}(^3\text{He},3n)$ $^{112}\text{Cd}(^3\text{He},4n)$ $^{113}\text{Cd}(^3\text{He},5n)$ $^{114}\text{Cd}(^3\text{He},6n)$ $^{116}\text{Cd}(^3\text{He},8n)$ $^{108}\text{Cd}(\alpha,n)$ $^{110}\text{Cd}(\alpha,3n)$ $^{111}\text{Cd}(\alpha,4n)$ $^{112}\text{Cd}(\alpha,5n)$ $^{113}\text{Cd}(\alpha,6n)$ $^{114}\text{Cd}(\alpha,7n)$ $^{116}\text{Cd}(\alpha,9n)$ $^{113}\text{In}(p,3n)$ $^{115}\text{In}(p,5n)$	-5620.67 -12596.3 -21990.35 -37572.03 -37572.03 -52412.37 -8959.43 -26198.3 -33173.93 -42567.98 -49106.73 -58149.64 -72989.98 -20351.3 -36664.46

Table 3: Activation cross sections of the $^{nat}\text{In}(p,xn)^{110}\text{Sn}$ reaction

CYRIC				LLN			
E (MeV)	ΔE (MeV)	σ (mbarn)	$\Delta\sigma$ (mbarn)	E (MeV)	ΔE (MeV)	σ (mbarn)	$\Delta\sigma$ (mbarn)
59.5	0.5	17.0	1.9	37.5	0.8	3.7	0.4
60.3	0.5	23.2	2.6	39.5	0.8	7.1	0.8
61.2	0.4	29.2	3.3	41.3	0.7	10.0	1.1
62.1	0.4	34.3	3.9	43.1	0.7	12.0	1.3
62.9	0.4	50.6	5.7	44.8	0.7	13.0	1.5
63.8	0.4	64.1	7.2	46.5	0.6	13.5	1.5
64.6	0.4	63.8	7.2	48.1	0.6	13.0	1.5
65.5	0.4	71.6	8.1	49.7	0.6	12.0	1.4
66.3	0.4	79.5	9.0	51.2	0.5	11.0	1.2
67.1	0.3	84.3	9.5	52.7	0.5	10.2	1.1
67.9	0.3	88.2	9.9	54.2	0.5	10.3	1.2
68.7	0.3	89.5	10.1	55.7	0.5	12.4	1.4
69.5	0.3	100.1	11.3	57.1	0.4	16.6	1.9
				58.4	0.4	23.2	2.6
				59.8	0.4	32.3	3.6
				61.1	0.4	42.4	4.8
				62.4	0.3	53.0	6.0
				63.7	0.3	62.3	7.0
				65.0	0.3	70.9	8.0

Table 4: Activation cross sections of the $^{nat}\text{Ag}(^3\text{He},xn)^{109,110,110g,111}\text{In}$ reactions

Energy		^{109}In		^{110m}In		^{110g}In		^{111}In	
$E \pm \Delta E$ (MeV)		$\sigma \pm \Delta\sigma$ (mbarn)							
10.4	0.6			0.3	0.1				
11.9	0.6	0.4	0.1	3.7	0.5				
13.3	0.5	1.6	0.2	18.0	2.1	0.5	6.6	1.0	0.4
14.7	0.5	6.8	0.6	41.0	4.7	1.2	19.1	2.4	0.6
15.9	0.5	18.4	1.5	36.6	4.8	2.2	38.4	2.3	0.8
17.1	0.5	54.2	3.2	36.7	4.7	3.2	55.8	3.5	1.3
18.2	0.5	87.4	5.0	29.3	4.2	3.4	60.4	6.7	1.5
19.3	0.4	126.1	7.0	21.1	3.5	3.5	60.8	5.8	1.6
20.3	0.4	164.2	9.1	18.9	3.3	3.3	58.7	7.1	1.5
22.2	0.4	230.7	12.6	14.7	2.7	2.7	48.2	4.4	1.3
23.1	0.4	247.1	13.5	9.7	2.5	2.3	40.8	4.8	1.5
24.1	0.3	262.4	14.3	11.7	2.5	1.9	34.2	3.7	0.9
25.0	0.3	272.2	14.9	11.4	2.4	1.7	29.4	6.5	2.0
26.6	0.3	277.8	15.1	9.3	2.1	1.4	23.0	4.9	2.0

Table 5: Activation cross sections of the natAg(α ,xn)^{109,110,110g,111}In reactions

Energy		¹⁰⁹ In		^{110m} In		^{110g} In		¹¹¹ In	
E \pm Δ E(MeV)		$\sigma \pm \Delta\sigma$ (mbarn)							
9.9	0.6			2.3	0.1				
11.9	0.6			31.2	1.8	5.6	0.4	0.3	0.02
12.0	0.5			27.2	1.6	4.4	0.3	0.3	0.03
13.6	0.5			128.0	7.5	39.3	2.3	2.5	0.14
15.3	0.5			255.6	14.9	106.8	6.2	63.3	3.4
16.7	0.5	33.8	4.7	338.8	19.7	221.7	12.9	264.6	14.3
18.2	0.4	115.0	13.2	282.8	16.5	260.7	15.2	445.7	24.1
19.5	0.4	266.0	30.2	275.6	16.0	278.8	16.3	679.1	36.7
20.8	0.4	374.5	42.2	140.7	8.2	208.3	12.2	800.2	43.3
22.0	0.4	495.8	56.0	124.5	7.3	163.9	9.6	982.5	53.1
23.2	0.3	533.2	60.0	59.8	3.5	104.3	6.1	991.9	53.6
24.3	0.3	629.4	70.9	62.8	3.7	82.1	4.8	1149.5	62.1
25.4	0.3	620.6	69.8	43.6	2.5	55.0	3.2	1114.2	60.2
26.5	0.3	695.9	78.2	45.9	2.7	61.3	3.6	1220.6	66.0